Anisotropy of elastic properties of SHS-synthesized porous titanium nickelide

A. A. Kozulin, *Candidate of Physical and Mathematical Sciences, Senior Researcher, kzln2015@yandex.ru*
A. V. Vetrova, *Post-Graduate Student, Engineer-Researcher*
Yu. F. Yasenchuk, *Candidate of Physical and Mathematical Sciences, Associate Professor, Senior Researcher*[1], *yayuri2008@gmail.com*
M. A. Kovaleva, *Student, Laboratory Assistant*[1]

[1]*National Research Tomsk State University, Tomsk, Russia.*

Samples of porous NiTi were obtained by the method of self-propagating high-temperature synthesis. The mechanical characteristics of the porous ones were studied by quasi-static compression. When the samples of porous titanium nickelide were subject to quasi-static compression, the deformation was of an elastic-plastic nature. Three characteristic types of the fracture surface under quasi-static compression of the porous SHS – TiNi alloy were identified: 1) ductile fracture of the austenite phase in the form of a cup relief, 2) brittle fracture accompanied by the formation of cleavage steps, 3) large areas of plastic shear deformation, on which cups and cleavage facets were nucleated. To determine the anisotropy of the porous TiNi alloy properties, the volume of the porous sample was simulated, and estimated calculations were carried out. Based on the results of reconstructing 3D neutron high resolution tomography of the porous volume of titanium nickelide and the numerical parameters of the model porous medium, an algorithm was developed for obtaining a solid-state 3D model of the porous framework for using in finite element calculations. The studied porous titanium nickelide alloy, as well as spongy bone tissues, was shown to have orthotropic elastic properties conditioned by the geometric features of the porous framework. The effective moduli of elasticity and shear for the porous volume of the material were determined. The calculation results of the elastic moduli for the studied model of porous titanium nickelide numerically agree with the results obtained by compressing the samples of porous TiNi. The porous TiNi alloy under uniaxial compression was established to be destroyed under the action of tangential shear stresses at an angle of 45 degrees to the direction of uniaxial compression.

Key words: Porous titanium nickelide; modeling; compression; orthotropy; anisotropy; 3D tomography; finite element method; elastic modulus; shear modulus.

DOI: 10.17580/nfm.2022.02.09

Introduction

Porous materials with a superelastic mechanical behavior can be found both among artificially created materials and in nature by the example of living tissues of the human body. Most of these materials have a complex porous structure, but the elastic properties and mechanical behavior of some special alloys are comparable with similar indicators of bone tissues [1], which in the aggregate has a favorable effect on the mechanical biocompatibility with the receptive bone tissue [2]. Therefore, during forced surgical interventions in orthopedics, porous materials based on titanium nickelide alloy (TiNi) occupy a special place among implantation materials [3, 4]. However, because of insufficient research, the applicability range of these materials is currently not fully clear, and some researchers even express doubt about the possibility of using porous titanium nickelide due to its insufficient bio-energy [5]. Nevertheless, owing to their unique properties, porous alloys based on titanium nickelide are an object that attracts special attention of specialists in the field of medical materials science because of their high interconnected porosity, permeability, superelasticity and manifestations of the shape memory effect when changing the temperature. Such combination of properties makes these materials promising for implantology due to the presence of through porosity and hydrophilic rough surface, which provide rapid invasion and regeneration of the bone tissue inside the porous implant.

Owing to the TiNi structure, formed by a directed combustion front during self-propagating high-temperature synthesis, the framework of the alloys having open porosity can exhibit anisotropy effects [6], which are divided into: a) anisotropy of mechanical properties, b) structural anisotropy [7], c) geometric anisotropy [8]. In the field of external load in a complex-stressed state, such multiscale systems deform super-elastically and accumulate damages at different scale levels, forming new geometric configurations of pores and bridges, thereby complicating the initial structure [9]. To make predictions about the mechanical similarity of the products made of the materials under study to biological tissues, numerical modelling is resorted to. One of the fundamental problems that arises when modeling such materials is the choice of determining equations that should describe all the aspects of the

mechanical behavior, including a deformation response in the presence of anisotropy of the mechanical properties. The used physico-mathematical models should consider both the mechanical behavior peculiarities in the local regions of the porosity framework and the pore space evolution in various loading conditions [10].

Vast literature is devoted to simulating the deformation of porous materials [11–15]. An effective approach to the study of such systems is the evolutionary methodology, developed by the authors [16–18]. From a mathematical viewpoint, the complete system of differential equations of continuum mechanics together with the defining relationships, describing the instable behavior of deformable solid bodies, represents complex systems of nonlinear equations. Nonlinear positive and negative feedbacks are explicitly specified in the system, which regulate the interaction between the material stress-strain state and the material response to loading in the form of damage accumulation on different scales and degradation of the strength properties. Such approach, undoubtedly, allows effectively describing the evolution of the properties of porous materials at different levels, including a localized accumulation of damages and superelastic deformations, strength degradation, formation of cracks of different scales, including main cracks leading to macroscopic destruction. However, representative volume elements are frequently prepared as geometric models with an artificially created porosity structure — close to ideal forms, or as phenomenological representations with continuous averaging that do not meet the peculiarities of the framework made during titanium nickelide SHS. Therefore, the purpose of this work is to study the facts of manifesting the properties anisotropy because of the geometric aspects of the porous framework, which must be considered explicitly in the geometric models when predicting the behavior of medical devices, made of titanium nickelide, acting as implants under operating conditions.

1. Materials and methods

1.1. Uniaxial compression of titanium nickelide samples

Samples cut out of cylindrical blanks made of porous titanium nickelide of the following sizes: the height of 120 mm; the diameter of 20 mm, were studied in the work. Blanks having 66% of porosity, average-sized through pores, ranging from 100 microns to 150 microns, were obtained by the SHS method in the mode of continuous laminar burning in the gas protective atmosphere of argon. When preparing the base Ni50 + + Ti50 mixtures to conduct SHS, the PTOM-2-grade titanium powder reduced by calcium hydride, with an average fraction size of 50 microns, and the PNK OT-4-grade nickel powder, with an average carbonyl fraction size of 50 microns, were used.

10 pieces of prismatic samples dimensioned $3 \times 3 \times 6$ mm^3 were cut out of the central part of the blank using electroerosion cutting for conducting experiments on uniaxial compression. The uniaxial compression experiment was carried out on an INSTRON 3369 testing machine by single loading up to destruction at a traverse travelling speed of 0.2 mm/min accompanied by fixing stress-strain curves to evaluate the physico-mechanical properties of porous TiNi.

1.2. Creation of a geometric solid-state three-dimensional model of porous titanium nickelide

To perform numerical calculations on determining the stress-strain state and finding elastic moduli at the initial stage of the computational experiment, a geometric model of the sample with an explicit porosity structure suitable for using in finite element calculations was prepared.

For this purpose, an algorithm for obtaining a solid-state CAD model based on *X*-ray tomography data was developed, including the following steps:

1. Obtaining the results of three-dimensional computer *X*-ray tomography in the form of a graphics files array with layerwise transverse and longitudinal sections of the porous titanium nickelide sample with a sufficient resolution and detailing. **Fig. 1** shows a single cross-section of the porous sample under study as an example. Since the material through porosity is within 60%, each section is represented as light-colored islands of the material against the black background.

The 3D tomography results were obtained in the neutron research center based on the IR-8 reactor of the RC "Kurchatov Institute". The equipment parameters were the monochromatic neutron flux energy of 46 keV, cross-sectional dimensions of the incident neutron beam of 75×75 mm^2, wavelength of 2.4 Å neutron flux density on the sample of 3.6×10^6 n/cm^2/s, spatial resolution of 200 μm, exposure of 0.8 s.

2. Processing of the tomography data. Using specialized software, the susceptibility degree of structural elements was adjusted on all the sections, and *X*-ray tomography artifacts in the form of noises were eliminated. After that, using the InVesalius 3.2 software, the obtained layered sections were sequentially glued while preserving the three-dimensional reconstruction of the porous cylindrical volume in the stl format. The image of the porous volume reconstruction is shown in **Fig. 2**. When creating and processing a three-dimensional model, the necessary condition was the exclusion of the fine porosity

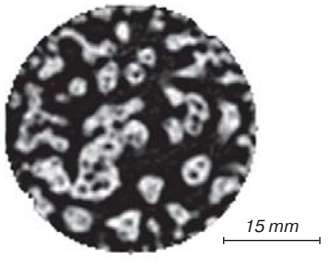

Fig. 1. Cross section of the porous sample made of the titanium nickelide alloy

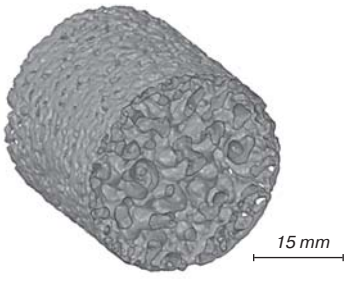

Fig. 2. Three-dimensional reconstruction of the porous volume in the form of the stl model

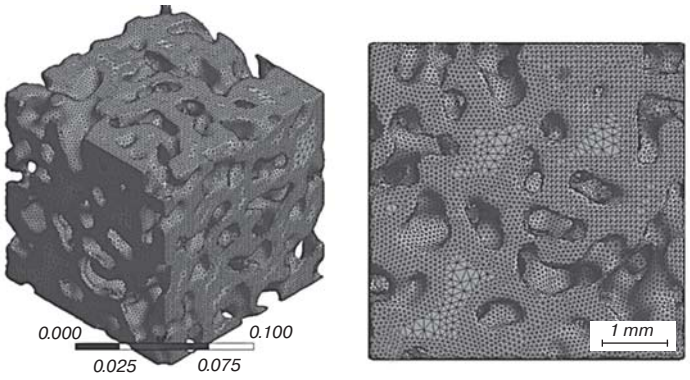

Fig. 3. Solid-state 3-D model of the porous framework

and inclusions on the walls and inside the framework. The presence of fine elements in the material structure made the model unsuitable for creating a computational finite-element mesh in the future.

3. The obtained stl model is not suitable for simulation, since it is not a solid body and consists only of a set of closed surfaces. This format was initially invented for additive technologies and is still successfully used in 3D printing. To create a solid-state model, the stl model was subject to conversion in the SpaceClaim solid-state modeling software package, as a result of which a volumetric 3D reconstruction of the cylindrical sample in the CAD format was obtained. It can be transferred to any engineering analysis software package that uses the finite element method.

4. To find the anisotropy of the properties, it is sufficient to examine samples of a representative volume in the form of a cube. At the same time, sample models were prepared by virtually cutting the porous volume out of the central part of the cylindrical model. The images of the samples are shown in **Fig. 3**.

1.3. Mathematical problem statement

The problem of determining the stress-strain state of the porous titanium nickelide sample under uniaxial loading and finding elastic moduli in three mutually perpendicular directions was solved.

The mathematical model for solving the set problem is represented by a system of differential equations of continuum mechanics in general terms, consisting of equilibrium equations (1), geometrical relationships (2) – Cauchy relations, defining relationships (3) in the form of Hooke's law. It was solved by the finite element method in the Lagrange approach in the Cartesian rectangular coordinate system (x_1, x_2, x_3):

$$\sigma_{ij,j} = 0, \quad (1)$$

$$\varepsilon_{kl} = \frac{1}{2}(u_{l,k} + u_{k,l}), \quad (2)$$

$$\sigma_{ij} = E_{ijkl}\varepsilon_{kl}^{el}, \quad (3)$$

$\sigma_{ij} = \sigma_{ji}$ $(i,j,k,l = 1, 2, 3)$ – components of the symmetric stress tensor; $\varepsilon_{ij} = \varepsilon_{ji}$ – components of the strain tensor; ε_{kl}^{el} – alues of elastic deformations; u_i and u_j – components of the displacement vector. The comma before the index means spatial coordinate differentiation.

The effective elastic moduli and the values of the Poisson's ratios in three mutually perpendicular directions were determined based on the stress-strain diagram, obtained numerically. For this purpose, boundary conditions for computational models were used, written in the form of:

$$\text{a) } u_{x_2}\Big|_{x_2 = 5\text{ mm}} = -u_0,\ u_{x_1,x_2,x_3}\Big|_{x_2 = 0\text{ mm}} = 0; \quad (4)$$

where $u_{x_2} = -u_0$ – shift along the x_2 axis by the value u_0 (mm) in the opposite direction from the direction of the axis of all the nodes of the model having the coordinate $x_2 = 5$; u_{x_1, x_2, x_3} – fixed (rigid) attachment of all the nodes with a coordinate $x_2 = 0$ mm.

u_0 (mm) – small shifts that do not lead to the appearance of plastic deformations in the volume:

$$\text{b) } u_{x_1}\Big|_{x_1 = 5\text{ mm}} = -u_0,\ u_{x_1,x_2,x_3}\Big|_{x_1 = 0\text{ mm}} = 0; \quad (5)$$

$$\text{c) } u_{x_3}\Big|_{x_3 = 5\text{ mm}} = -u_0,\ u_{x_1,x_2,x_3}\Big|_{x_3 = 0\text{ mm}} = 0. \quad (6)$$

When performing the calculations, the porous framework material of the studied samples was assumed to have isotropy properties. And the material properties, characteristic of polycrystalline titanium nickelide, were used as the initial parameters of the material, whose Young modulus of elasticity was $E = 74$ GPa, Poisson's ratio was $\nu = 0.3$, shear modulus was $G = 28$ GPa, density was $\rho = 6650$ kg/m^3.

2. Results

2.1. Results of quasi-static uniaxial compression of the porous titanium nickelide samples

During quasi-static uniaxial compression of 5 porous titanium nickelide samples sized 6×3×3 mm^3 up to the destruction, deformation dependences were obtained **(Fig. 4)**. The table shows the average values of the sought quantities, which have confidence intervals after statistical averaging with respect to testing several samples.

The loading diagrams for all the tested samples are qualitatively similar. Based on the analysis of the deformation curves, it is apparent that there are no yield point areas associated with the martensitic transition (MT) characteristic of monolithic alloys based on TiNi. Therefore, the deformation curves have a form that is peculiar to elastic-plastic deformation along with strengthening. Superelasticity effects are apparently manifested in local regions of deformation localization on the porous frame bridges. In the area of softening, the steps during destruction indicate the non-simultaneous destruction of the porous frame bridges.

In [19], samples of spongy bone were examined by uniaxial compression. The spongy bone under compression partially decays and acquires a fibrous structure. The maximum compression stress when the destruction begins was 52 ± 3 MPa under the deformation of 3.5–4%. The

strain diagram before destruction is elastic in nature. The obtained experimental deformation dependences of porous TiNi and spongy bone samples [19] are qualitatively similar, despite the fundamental differences in the deformation micromechanics of the compared materials.

For the comparative analysis, **Table 1** shows the data on the physical and mechanical properties of Ti-based porous alloys, obtained by other authors, intended for use in implants.

Comparison of the experimental results with the literature data confirms the fact that porous alloys obtained by the SHS method have stiffness, strength and plasticity values under compression that are not lower than the values obtained by other authors [1, 20–26] on titanium-containing materials, obtained by other methods. In [1], Ti6Al4V-based alloys have porosity ranging within 60–85% with pore sizes starting from 250 μm in case of the elastic modulus variation from 0.5 to 3 GPa. At the same time, the authors claim that such characteristics are sufficient for mechanical compatibility when using porous alloys as implants while working jointly with the trabecular bone; however, the next method aimed at improving the mechanical compatibility consists in reducing the pore sizes of while maintaining porosity values. Based on this, it can be argued that the TiNi-based porous alloy, obtained by us, with porosity indices of 66%, pore sizes of up to 150 microns, Young modulus equal to 3.2 GPa corresponds to the mechanical parameters of the trabecular bone and the materials of many commercially available implants [1]. This is a prerequisite for their mechanical biocompatibility.

2.2. Peculiarities of fracture surfacesofporous SHS – TiNi alloys under quasi-static compression

The destruction nature of the porous framework walls is mixed, the viscous fracture being predominant. A large number of areas of the stepwise viscous shear in combination with a cup relief of a ductile fracture were found on the fracture surfaces. This confirms the assumption that the effect of superelasticity is manifested only in local regions of deformation localization. There are areas with brittle fracture facets, along which cracks pass, as well as cracks in the surface shell **(Fig. 5, *a*)**.

The areas with brittle fracture facets and a large number of cracks spreading normally to the main fracture surface belong to the brittle Ti_2Ni phase distributed along the boundaries of austenite grains. Large surfaces of shear

Table 1

Physical and mechanical characteristics of porous alloys intended for manufacturing implants

Composition	*E*, GPa	σ_e, MPa	$\sigma_в$, MPa	ε_{tot}, %	Res.
$Ti_{50}Ni_{50}$	4.5 ± 0.3	75 ± 7	200 ± 18	15 ± 1	Orig.
$Ti_{50}Ni_{50}$	0.8; 1	80; 101	109; 122	18; 22	[20, 21]
$Ti_{50}Ni_{50}$	4	200	240 ± 14	7.75 ± 0,1	[22]
$Ti_{55}Ni_{45}$	1,4–1,9	30	130; 220	15-20	[23, 24]
$Ti_{45}Ni_{55}$	4.6; 4.25	80; 85	462; 210	11; 17	[25, 26]
Ti_6Al_4V	0.5-3± 0.5	–	–	–	[1]

Notes: σ_e is the elastic limit; $\sigma_в$ is the tensile strength in accordance with the loading scheme; *E* is the Young modulus; ε_{tot} is the total strain-to-fracture.

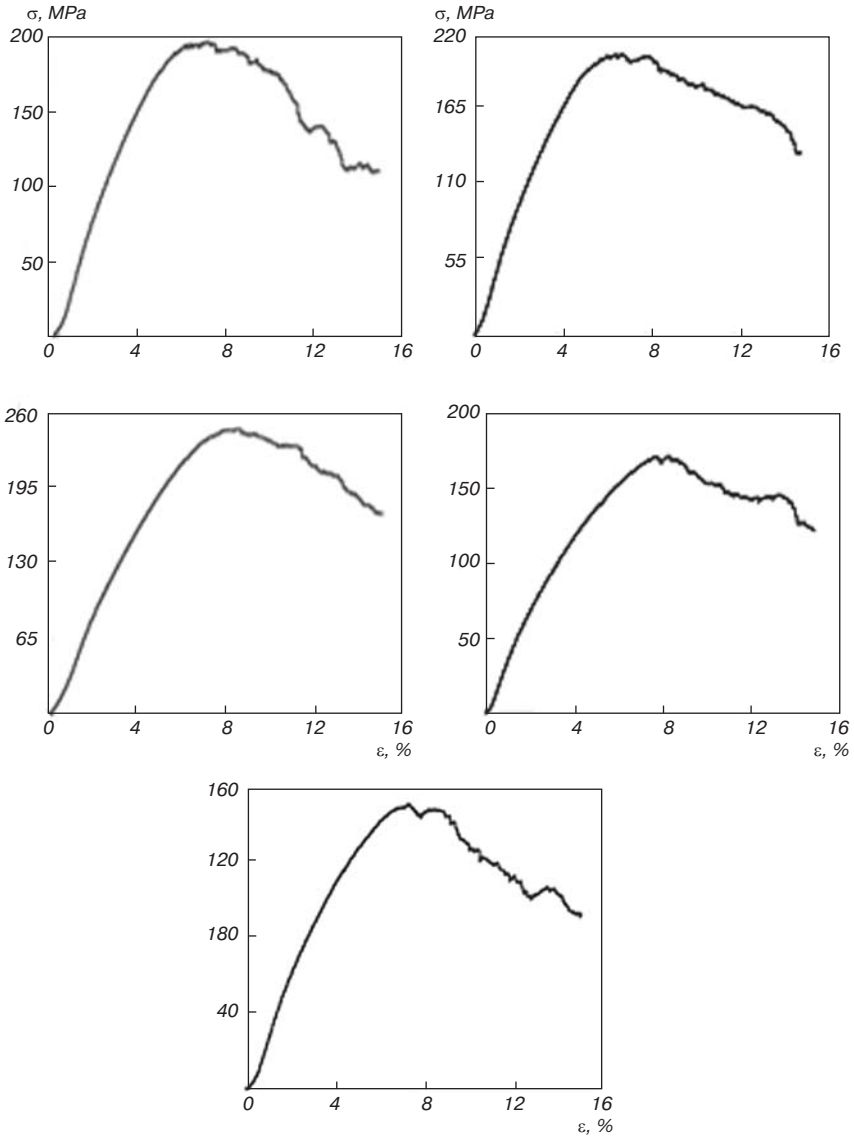

Fig. 4. Typical experimental strain diagrams obtained by uniaxial quasi-static compression of porous SHS alloys based on titanium nickelide

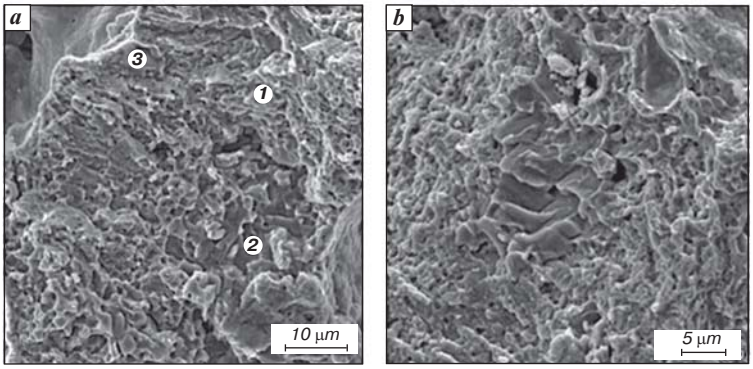

Fig. 5. Micrographs of fracture surfaces:
a – a general view of the fracture surface of the porous framework wall;
b – a fragment of the fracture surface with a central section of a brittle stepped chip surrounded by a pit relief of the ductile fracture

deformation of the austenitic phase have a residual pit relief. An area of a stepped chip of the brittle phase is in the center of the ductile fracture surface of the austenitic phase with a cup-shaped relief **(Fig. 5, *b*).**

Summarizing the results, obtained by the quasi–static compression of the porous SHS – TiNi alloy, three characteristic types of the fracture surface of the bridges can be distinguished. The first is ductile fracture of the austenitic phase in the form of a cup relief. The second is brittle fracture accompanied by the formation of cleavage steps. The third is large areas of plastic shear deformation on which cups and facets of cleavage originate. The predominant fracture type in the porous framework walls is ductile, which indicates the predominance of the austenitic TiNi(B2) phase at the initial stage of porous titanium nickelide destruction.

2.3. Simulation results of the geometric solid-state 3-D model of porous titanium nickelide.

The estimated calculations were performed to determine the anisotropy of the porous sample properties. For this purpose, the effective elastic moduli for the porous volume of the material were determined. A $5 \times 5 \times 5$ mm^3 cube obtained on the basis of tomography results was considered.

Table 2
Values of effective elastic moduli for the material porous volume obtained experimentally and numerically by uniaxial compression

Elastic modulus	Calculated value	Experimental values
Young modulus E_1, GPa	2.98	–
Young modulus E_2, GPa	3.24	3.2
Young modulus E_3, GPa	3.01	–
Shear modulus G_{12}, GPa	1.21	–
Shear modulus G_{23}, GPa	1.31	–
Shear modulus G_{31}, GPa	1.22	–
Poisson's ratio ν_{12}	0.231	–
Poisson's ratio ν_{13}	0.2375	–
Poisson's ratio ν_{23}	0.2332	–

When simulating, a representative volume was selected from a variety of prepared CAD models of different shapes, orientations and sizes, because sufficiently large samples did not allow simulating due to the complexity of calculations and computing power overload along with a multiple increase in the estimated time. The results obtained on different smaller volumes mismatched and did not reflect the material porous properties in its different sections. Based on the selected series of representative volumes, the results were identical with an acceptable level of error. The computational experiments conducted on the selected representative volumes of $5 \times 5 \times 5$ mm^3, this time in the linear approximation, allow identifying the deformation localization peculiarities in the studied porous sample in the framework sections characteristic of the porous frame bridges. **Fig. 6, *a*** shows the areas of the stress concentration and strain localization where equivalent stress values that are close to the conventional yield strength for a monolithic material are reached. **Fig. 6, *b*, *c*** presents the values of equivalent deformations corresponding to such moment of distributing equivalent stresses. The regions of the critical von Mises stress concentration are located in the areas with the maximum curvature of the framework surface; they are shown in light colors other than blue.

The distribution of stress-and-strain fields, obtained as a result of the computational experiment, corresponds to the localization of sources of damage accumulation and fracture zones during compression up to the porous TiNi alloy destruction. The general direction of the fracture surfaces of the porous alloy under the action of tangential shear stresses is at an angle of 45 deg. to the uniaxial compression direction. In this way, it is possible to claim that the porous TiNi alloy under uniaxial compression is destroyed according to the standard shear mechanism, described by the deformable solid mechanics.

A series of the performed computational experiments on the axial compression and shear of the representative volumes of the porous sample in three mutually perpendicular directions is sufficient to determine the values of effective elastic moduli. In this case, the properties are considered orthotropic, which is a special case of anisotropy.

Table 2 shows the calculation results, where figures 1, 2, 3 correspond to the Cartesian coordinates x_1, x_2, x_3. Coordinate axis 2 corresponds to the direction of the combustion wave front in the SHS synthesis, the axes with indices 1 and 3 lie in the plane that is orthogonal to the front. The effectiveness of using the model is confirmed by comparing the experimental and calculated data on the Young modulus.

Owing to the porosity, the estimated effective properties of the volume under consideration turned out to be less than the properties of the original monolithic material. When analyzing the results presented in **Table 2**, it was

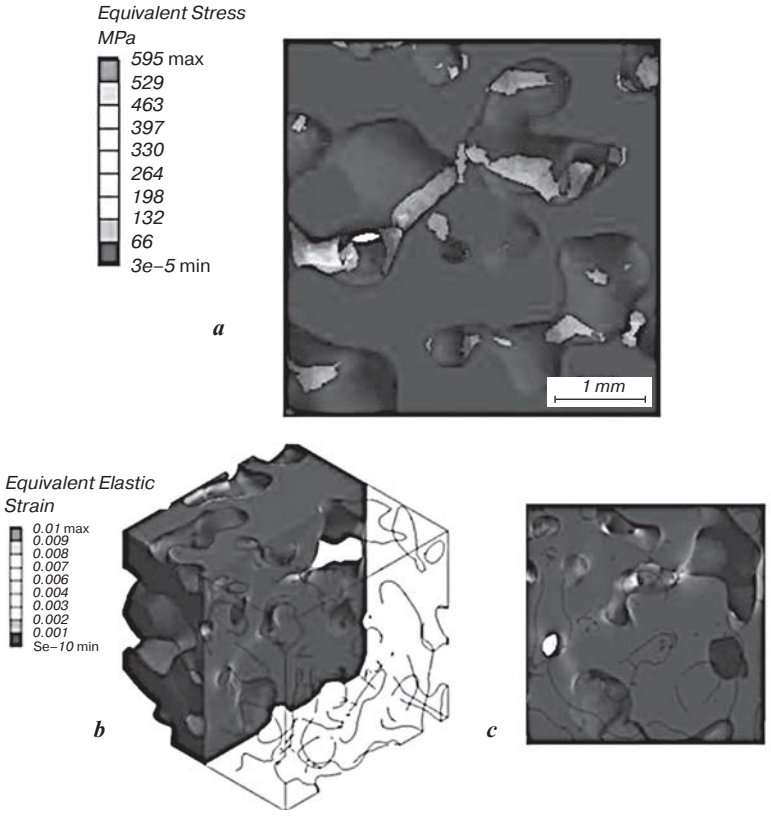

Fig. 6. Representative results of the numerical simulation:
a – distribution of equivalent stresses in the volume of the model under compression along the *Y* axis (view of one of the surfaces of the volume under study).
Distribution of equivalent deformations in the volume of the model under compression along the x_2 axis:
b – model isometry with a cross section;
c – cross section view $YZ|_{x_3 = 2.5\ \text{mm}}$

found that the values of the elastic moduli varied, depending on the direction of the coordinate axes. The maximum value is realized along the x2 axis (along the direction of the combustion wave front) and is equal to 3.24 GPa, the minimum value is equal to 98 GPa along the x1 axis. The shear moduli and Poisson's ratios have a similar tendency to change values, depending on the direction of the axes. Based on the presented results, it may be concluded that the studied porous volume has the orthotropy of the elastic properties because of the geometry peculiarities of the porous framework, formed during the synthesis. The effective density value of the considered porous representative volume is equal to 2193 kg/m^3, which is 66 % less than the monolithic material density. The results, obtained on the basis of different models, having the same dimensions within the framework of volume representativeness, vary within the acceptable error threshold of up to 5%.

Conclusion

During quasi-static compression of the porous titanium nickelide samples, the deformation was established to have an elastic-plastic nature. The porous frame bridges were destroyed viscously and non-simultaneously, which was characterized by a stepwise form of the softening stage. When analyzing the theoretical and experimental results, the cause of the porous TiNi-based alloy destruction under uniaxial compression was established to be localized deformations in the region of thinning the frame bridges, which becomes a defect accumulation site under the action of tangential shear stresses at an angle of 45 degrees to the uniaxial compression direction.

Three characteristic types of the fracture surface under quasi-static compression of the porous SHS-TiNi alloy were distinguished: 1) viscous destruction of the austenitic phase in the form of a cup relief, 2) brittle destruction accompanied by the formation of cleavage steps, 3) large areas of plastic shear deformation on which cups and facets of cleavage originate. The predominant fracture type in the porous framework walls was established to be viscous, which indicates the predominance of the austenitic TiNi(B2) phase at the initial stage of porous titanium nickelide destruction.

An algorithm for obtaining a solid-state model of the porous framework that is suitable for using in finite element calculations was developed. The effective elastic moduli for the studied porous volume of the material were determined based on numerical modeling. The studied porous volume was shown to have orthotropic elastic properties due to the geometry peculiarities of the porous framework, formed during the synthesis. Therefore, this fact is to be taken into account when predicting the behavior of products made of this material under operating conditions. Introducing the anisotropy of the properties into engineering calculations when designing medical devices should provide more accurate results when assessing strength or topological optimization and forecasting biomechanical compatibility. The values of the calculated Young modulus for the studied model of porous titanium nickelide range from 2.98 to 3.24 GPa and correspond to the results obtained under the experimental compression of the porous TiNi samples.

The research was carried out with financial support of the Russian Science Foundation under the Grant No. 22-72-10037, https://rscf.ru/project/22-72-10037/.

References

1. Grunsven W., Goodall R., Reilly G. C. Highly Porous Titanium Alloy: Fabrication and Mechanical Properties. *Journal of Biomechanics*. Vol. 45. S339.

2. Uzunyan N. A., Olesova V. N., Lebedenko I. Yu., Khafizov R. G., Filonov M. R., Ivanov A. S. Experimental Study of The Dynamics of Osseointegration of the Dental Implants

of Superelastic Titanium Alloys. *Rossiyskiy Vestnik Dentalnoy Implantologii*. 2018. Vol. 39-40, Iss. 1-2. pp. 8–11.

3. Marchenko E., Yasenchuk Yu., Avdeeva D., Baigonakova G., Gyunter S., Iuzhakova M. Deformation Behavior, Fatigue and Fracture Surface Microstructure of Porous Titanium Nickelide. *Micro and Nanosystems*. 2021. Vol. 13, Iss. 4. pp. 442–447.

4. Yasenchuk Yu. F., Marchenko E. S., Baigonakova G. A., Gyunter S. V., Kokorev O. V., Gunther V. E., Chekalkin T. L., Topol`nickij E. B., Obrosov A., Kang J.-H. Study on Tensile, Bending, Fatigue, and In Vivo Behavior of Porous SHS-TiNi Alloy Used as a Bone Substitute. *Biomedical Materials*. 2021. Vol. 6, Iss. 2. 021001

5. Uzunyan N. A. Substantiation of the Use of New Domestic Superelastic Titanium Alloys in Dental Implantology (Experimental Clinical Study). A Dissertation ... Doctor of Medical Sciences. Moscow, 2019. 179 p.

6. Gunther V. E., Yasenchuk Yu. F., Gyunter S. V., Marchenko E. S., Iuzhakov M. M. Biocompatibility of Porous SHS-TiNi. *Materials Science Forum*. 2019. Vol. 970. pp. 320–327.

7. Kang J., Dong E., Li D., Dong S., Zhang C., Wang L. Anisotropy Characteristics of Microstructures for Bone Substitutes and Porous Implants with Application of Additive Manufacturing in Orthopaedic. *Materials & Design*. 2020. Vol. 191. 108608.

8. Gómez S., Vlad M. D., López J., Fernández E. Design and Properties of 3D Scaffolds for Bone Tissue Engineering. *Acta Biomaterialia*. 2016. Vol. 42. pp. 341–350.

9. Marchenko E. S., Yasenchuk Yu. F., Gyunter S. V., Baigonakova G. A., Gunther V. E., Chekalkin T. L., Weiss S., Obrosov A., Dubovikov K. M. Structural-Phase Surface Composition of Porous TiNi Produced by SHS. *Materials Research Express*. 2019. Vol. 6, Iss. 11. 1165b1.

10. Smolin I. Yu., Makarov P. V., Eremin M. O., Matyko K. S. Numerical Simulation of Mesomechanical Behavior of Porous Brittle Materials. *Procedia Structural Integrity*. 2016. Vol. 2. pp. 3353–3360.

11. Bruno G., Efremov A. M., Levandovskyi A. N., Clausen B. Connecting the Macro- and Microstrain Responses in Technical Porous Ceramics: Modeling and Experimental Validations. *Journal of Materials Science*. 2011. Vol. 46, Iss. 1. pp. 161–173.

12. Roberts A., Garboczi E. Elastic Properties of Model Porous Ceramics. *Journal of the American Ceramic Society*. 2000. Vol. 83, Iss. 12. pp. 3041–3048.

13. Torquato S. Random Heterogeneous Media: Microstructure and Improved Bounds on Elastic Properties. *Applied Mechanics Reviews*. 1991. Vol. 44, Iss. 2. pp. 37–76.

14. Konovalenko I. S., Smolin A. Y., Korostelev S. Y., Psakh'e S. G. Dependence of the Macroscopic Elastic Properties of Porous Media on the Parameters of a Stochastic Spatial Pore Distribution. *Technical Physics*. 2009. Vol. 54, Iss. 5. pp. 758–761.

15. Smolin I. Yu., Eremin M. O., Makarov P. V., Evtushenko E. P., Kulkov S. N., Buyakova S. P. Brittle Porous Material Mesovolume Structure Models and Simulation of their Mechanical Properties. *AIP Conference Proceedings*. 2014. Vol. 1623. 595.

16. Makarov P. V. Evolutionary Nature of Destruction of Solids and Media. *Physical Mesomechanics*. Vol. 10, Iss. 3–4. pp. 134–147.

17. Makarov P. V. Mathematical Theory of Evolution of Loaded Solids and Media. *Physical Mesomechanics*. 2008. Vol. 11, Iss. 5–6. pp. 213–227.

18. Kostandov Y. A., Makarov P. V., Eremin M. O., Smolin I. Y., Shipovskii, I. E. Fracture of Compressed Brittle Bodies with a Crack. *International Applied Mechanics*. 2013. Vol. 49, Iss. 1. pp. 95–101.

19. Medical Materials and Implants with Shape Memory. In 14 vols. Ed. by Gyunter V. E. Tomsk: NII Meditsinskikh Materialov i Implantov s Pamyatyu Formy SFTI pri TGU, 2011. 533 p.

20. Guo Z., Xie H., Dai F., Qiang H., Rong L., Chen P., Huang F. Compressive Behavior of 64% Porosity NiTi Alloy: An Experimental Study. *Materials Science and Engineering: A*. 2009. Vol. 515, Iss. 1-2. pp. 117–130.

21. Barrabés M., Sevilla P., Planell J. A., Gil F. J. Mechanical Properties of Nickel–Titanium Foams for Reconstructive Orthopaedics. *Materials Science and Engineering: C*. 2008. Vol. 28, Iss. 1. pp. 23–27.

22. Wisutmethangoon S., Denmud N., Sikong L. Characteristics and Compressive Properties of Porous NiTi Alloy Synthesized by SHS Technique. *Materials Science and Engineering: A*. 2009. Vol. 515, Iss. 1-2. pp. 93–97.

23. Resnina N., Belyaev S., Voronkov A., Gracheva A. Mechanical Behaviour and Functional Properties of Porous Ti-45 at.% Ni Alloy Produced by Self-Propagating High-Temperature Synthesis. *Smart Materials and Structures*. 2016. Vol. 25, Iss. 5. 055018.

24. Resnina N., Belyaev S., Voronkov A. Functional Properties of Porous Ti-48.0 at.% Ni Shape Memory Alloy Produced by Self-Propagating High-Temperature Synthesis. *Journal of Materials Engineering and Performance*. 2018. Vol. 27, Iss. 3. pp. 1257–1264.

25. Kaya M., Orhan N., Tosun G. The Effect of the Combustion Channels on the Compressive Strength of Porous NiTi Shape Memory Alloy Fabricated by SHS as Implant Material. *Current Opinion in Solid State and Materials Science*. 2010. Vol. 14, Iss. 1. pp. 21–25.

26. Li Y.-H., Rong L.-J., Li Y.-Y.. Compressive Property of Porous NiTi Alloy Synthesized by Combustion Synthesis. *Journal of Alloys and Compounds*. 2002. Vol. 345, Iss. 1-2. pp. 271–274. NFM